GEOLOGICA BELGICA (2005) 8/4: 20-34.

TIMING AND DURATION OF THE PROGRESSIVE DEFORMATION OF THE BRABANT MASSIF, BELGIUM

Timothy N. DEBACKER[1,3], Stijn DEWAELE[2], Manuel SINTUBIN[1], Jacques VERNIERS[3], Philippe MUCHEZ[2] & Ariël BOVEN[4]

(9 figures, 1 table)

1. Structural Geology & Tectonics Group, Katholieke Universiteit Leuven, Redingenstraat 16, B-3000 Leuven.
2. Geodynamics & Geofluids Research Group, Katholieke Universiteit Leuven, Celestijnenlaan 200C, B-3000 Leuven.
3. Onderzoekseenheid Paleontologie, Vakgroep Geologie en Bodemkunde, Universiteit Gent, Krijgslaan 281, S8, B-9000
4. Eenheid Geochronologie, Vrije Universiteit Brussel, Pleinlaan 2, B-1050 Brussel

ABSTRACT. A comparison of structural, geophysical, metamorphic, stratigraphical and sedimentological data suggests that the progressive deformation of the Brabant Massif, the Brabantian orogeny, is more diachronous than commonly thought. Apparently, the Cambrian core of the massif was already deforming by the late Llandovery, whereas the Ludlow deposits below the angular unconformity probably did not experience deformation prior to the late Pragian. Hence, the Brabant Massif experienced a long-lived deformation history, lasting for at least ~30 Ma. The slow, progressive deformation model is supported by $^{40}Ar/^{39}Ar$ dating of syn- to post-cleavage, metamorphic muscovite/sericite grains. The $^{40}Ar/^{39}Ar$ spectra indicate that episodic metamorphic fluid circulation occurred between ~426 and ~393 Ma. This time interval corresponds to that of the progressive deformation inferred from structural, geophysical, metamorphic, stratigraphical and sedimentological observations.

KEYWORDS. Brabant Massif, burial metamorphism, compressional wedge, foreland basin, Lower Palaeozoic, progressive deformation, $^{40}Ar/^{39}Ar$ dating

1. Introduction

The Lower Palaeozoic Brabant Massif (Figs 1 & 2) forms the southeastern part of the Anglo-Brabant Deformation Belt, situated within the eastern Avalonia Terrane Assemblage. The deformed, low-grade metamorphic deposits of the massif are separated by an angular unconformity from overlying, undeformed, diagenetic Givetian and younger deposits (De Vos *et al.*, 1993a; Van Grootel *et al.*, 1997; Verniers *et al.*, 2002; Bultynck *et al.*, 1991; Gerrienne *et al.*, 2004). In the outcrop areas along the southern rim of the massif, the youngest deformed deposits have a Gorstian (early Ludlow) age (Louwye *et al.*, 1992). Hence, deformation within the Brabant Massif, or the Brabantian orogeny, is unanimously considered to have taken place sometime between the Gorstian and the Givetian (e.g. Fourmarier, 1921, 1931, 1954; Mortelmans, 1955; Beugnies, 1964; Legrand, 1967; Verniers & Van Grootel, 1991; Van Grootel *et al.*, 1997). However, suggestions about the exact timing of deformation widely differ: late Ludlow (Beugnies, 1964), late Silurian (Legrand, 1968), Lochkovian (Michot, 1978; Verniers & Van Grootel, 1991) and Emsian (Fourmarier, 1931, 1954; Mortelmans, 1955; Verniers & Van Grootel, 1991). In addition, also the number of deformation phases has been debated (e.g. Legrand, 1967; Michot, 1978; Verniers & Van Grootel, 1991; Giese *et al.*, 1997).

During the last three decades of the 20th century,

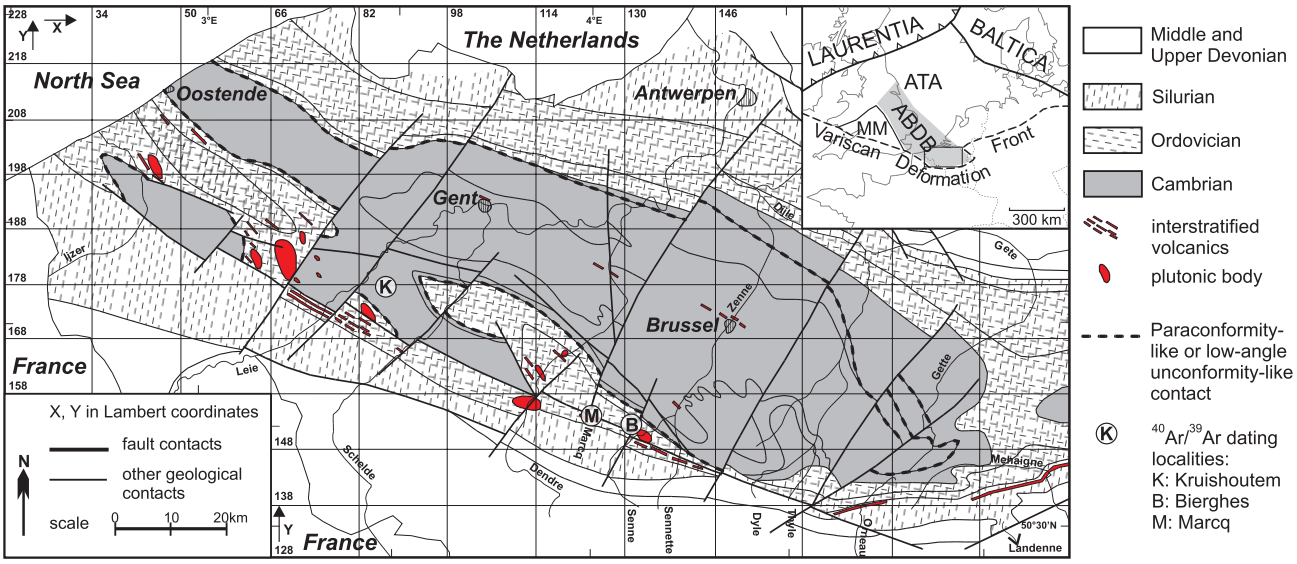

Fig. 1: Geological subcrop map of the Brabant Massif (after De Vos *et al.*, 1993a; Van Grootel *et al.*, 1997), with an inset (upper right) showing the position of the Brabant Massif within the Anglo-Brabant Deformation Belt (ABDB) along the NE-side of the Midlands Microcraton (MM) in the context of Avalonia (Avalonia Terrane Assemblage: ATA), Baltica and Laurentia. The $^{40}Ar/^{39}Ar$ dating sampling localities are indicated. The paraconformity-like or low-angle unconformity-like contact surrounding the Lower Cambrian core of the massif, inferred from the subcrop map of De Vos *et al.* (1993a), corresponds to the Asquempont Detachment System and consists of one or more pre-cleavage low-angle extensional detachments, such as the Asquempont fault (Debacker *et al.*, in press; cf. Debacker *et al.*, 2003).

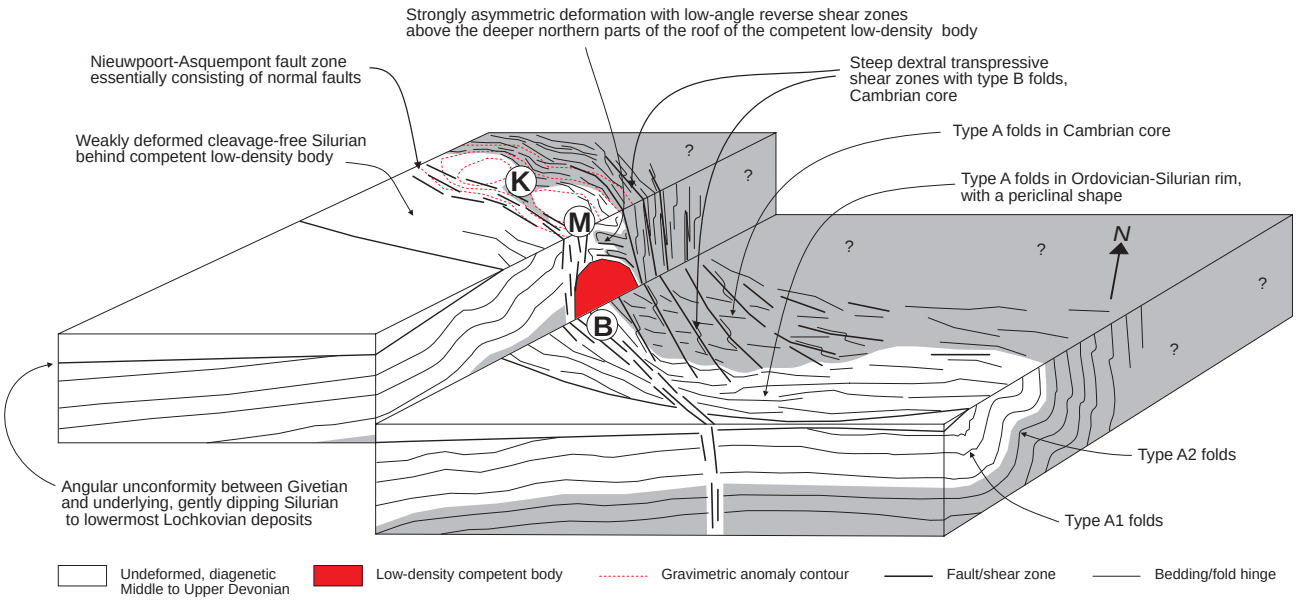

Fig. 2: Conceptual block diagram of the deformation geometry and kinematics in the southern part of the Brabant Massif (Debacker, 2001; see also Fig. 1). The western part of the block diagram is uplifted in order to show the deformation style in the direct surroundings of the low-density gravimetric anomaly body, which, during deformation, behaved as a competent body (cf. De Vos, 1997; Sintubin, 1999). The approximate $^{40}Ar/^{39}Ar$ dating sampling localities are also indicated (K: Kruishoutem; B: Bierghes; M: Marcq).

several researchers attempted to further constrain the deformation age of the Brabant Massif by means of radiometric dating methods. Unfortunately, these radiometric ages often added more confusion. Instead of narrowing down the possible age-range of deformation, these ages suggested an even bigger time-interval. Within the Cambrian core, ages of 450 ± 21 Ma (Rb-Sr whole-rock; Michot, 1976) and 401 ± 13 Ma (Rb/Sr on newly formed biotite; Michot *et al.*, 1973) were obtained, both of which are considered to reflect cleavage development (André *et al.*, 1981). In contrast, Rb-Sr whole-rock ages on Ordovician magmatic rocks yielded ages of 376 ± 24 Ma and 404 ± 19 Ma at Izegem (Andre *et al.*, 1981), 373 ± 11 Ma at Bierghes (André & Deutsch, 1985) and 379 ± 13 Ma at Deerlijk-Harelbeke (André & Deutsch, 1985) and Rb-Sr internal mineral isochrones yielded 372 ± 13 Ma and 375 ± 14 Ma at Quenast (André & Deutsch, 1985). Although these were initially considered to reflect the same tectonometamorphic event as that dated within the Cambrian core (André *et al.*, 1981), they have later been re-interpreted as resulting from a Sr isotopic resetting during strike-slip deformation (André & Deutsch, 1985). At that time, however, the geology of the Brabant Massif was much less well understood as it is today.

Since then, many advances have been made in the understanding of the stratigraphy, sedimentology, metamorphism and structural architecture of the Brabant Massif. In addition, recently some single-grain mica $^{40}Ar/^{39}Ar$-ages were obtained from several places within the massif (Dewaele *et al.*, 2002; Dewaele, 2004). In the present paper we integrate these radiometric data with stratigraphic, sedimentological, metamorphic, structural and geophysical data in order to get a better insight in the deformation history of the Brabant Massif. For this purpose, first an outline is given of the structural architecture and the kinematic constraints of the deformation within the Brabant Massif.

2. Structure and single progressive deformation

2.1. Structural outcrop data

2.1.1. Cleavage/fold relationships

Detailed field studies have shown that throughout the outcrop areas of the Brabant Massif there is only evidence for one single progressive deformation, which mainly resulted in the development of folds with a cogenetic cleavage (Sintubin *et al.*, 1998; Sintubin, 1997a, 1999; Debacker, 1999, 2001; Debacker *et al.*, 1999, 2004a).

On the basis of the cleavage/bedding relationships within the Brabant Massif, two main fold types can be distinguished, each occupying particular areas (Fig. 2; cf. Sintubin, 1997a, 1999). Importantly, both fold types are cogenetic with cleavage (e.g. Sintubin *et al.*, 1998; Debacker *et al.*, 1999, 2004a). The Lower Cambrian core of the massif, interpreted as a steep belt (Sintubin, 1999), is characterised by a generally sub-vertical to steeply dipping bedding, a sub-vertical to steeply dipping cleavage, and the common occurrence of steeply plunging folds (Sintubin, 1997a, 1999; Sintubin *et al.*, 1998; Debacker, 2001; Debacker *et al.*, 2004a), labelled type B folds (Debacker *et al.*, 2004a; Lembeek fold type of Sintubin, 1997a). In contrast, the Ordovician-Silurian southern part of the massif is characterised by a steep to moderately N-dipping cleavage and sub-horizontal to gently plunging folds (Sintubin, 1997a, 1999; Debacker, 2001; Debacker *et al.*, 2004a), labelled type A folds (Debacker *et al.*, 2004a). Two sub-types of type A folds can be distinguished, labelled type A1 and type A2 folds (Fig. 2; Debacker, 2001). Type A1 folds (Ronquières fold type of Sintubin, 1997a), observed within the Silurian deposits above the lower Wenlock Corroy Formation (Debacker, 2001, 2002), are gentle to close, upright to slightly asymmetric folds, with well-developed convergent cleavage fans (e.g. Legrand, 1967; Debacker *et al.*, 1999; Debacker, 2001). Type A2 folds (partly corresponding to the Fauquez fold type of Sintubin, 1997a), observed within the Ordovician and Silurian deposits up to the lower Wenlock Corroy Formation, are open to tight folds, usually with a stepfold geometry and a S-verging asymmetry, having a parallel to slightly divergently fanning axial planar cleavage (e.g. Debacker *et al.*, 2001, 2003).

Although previously the Asquempont fault (Fig. 1) was considered a major tectonic boundary between the steep Cambrian core and the Ordovician-Silurian southern part of the Brabant Massif, and was held responsible for the division between the type B and type A folds (e.g. Sintubin *et al.*, 1998; Sintubin, 1999), recent field observations in the

southern parts of the Cambrian core have demonstrated a gradual transition between the type A folds and the type B folds (Debacker, 2001; Debacker *et al*., 2004a, in press). This transition, which is unrelated to the Asquempont fault (cf. Debacker *et al*., 2003), occurs repeatedly and gradually in NW-SE-trending zones of several hectometres to several kilometres wide. Apparently, these zones, in which also the type B folds occur, coincide with NW-SE-trending aeromagnetic lineaments (Fig. 2; see below).

2.2.2. Faults

Although previously several authors have advocated the importance of reverse faults in the deformation history of the Brabant Massif (e.g. Mortelmans, 1955), recent studies have not found evidence for this (e.g. Giese *et al*., 1997). On the contrary, it appears that reverse faults are relatively scarce and only have a minor effect on the architecture and stratigraphic distribution as compared to normal faults (Debacker, 2001; Debacker *et al*., 2003, 2004b). On the basis of fault kinematics and the relationship with other deformation features, three main fault types can be distinguished (Debacker, 2001; Debacker *et al*., 2003, 2004b).

The first type is represented by the Asquempont fault (Fig. 1), the oldest fault recognised thus far in the Brabant Massif. Instead of representing an important steep reverse fault between the Lower Cambrian core and the Ordovician southern part, this fault has recently been redefined as a pre-cleavage and pre-folding low-angle extensional detachment (Debacker *et al*., 2003, 2004b). Judging from the hanging wall stratigraphy, this fault formed between the Caradoc and the timing of cleavage development.

The second fault type is represented by reverse faults. These usually have a minor stratigraphic displacement, and a position, geometry and kinematics suggestive of a close relationship with folding and cleavage development. Two subtypes can be distinguished (Debacker, 2001). The first and most common subtype consists of relatively small, low-angle reverse faults, commonly without significant wall-rock deformation or fault-rock development. These often occur along fold axial surfaces, or as fold accommodation structures within fold hinge zones. Probably, these faults initiated during folding, but experienced part of the displacement and fault propagation after cleavage development. The second subtype is represented by a syn-cleavage, low-angle reverse shear zone, intimately related with folding and cleavage development (Debacker, 1999; Piessens *et al*., 2002). This shear zone, affecting the Lower Ordovician deposits of the Marcq area, is situated above an important negative bouguer anomaly in the SW-part of the Brabant Massif (Fig. 2; De Meyer, 1983, 1984; Everaerts *et al*., 1996; see below). Although having a relatively small stratigraphic displacement (Debacker, 1999; cf. Vanguestaine, unpub. data 2001) this shear zone is characterised by an extensive synkinematic alteration (sericitisation, silicification and chloritisation) and mineralization (Piessens *et al*., 2000a, 2002; Dewaele, 2004). This synkinematic alteration yields important $^{40}Ar/^{39}Ar$ ages (Dewaele *et al*., 2002; see below).

The third fault type consists of subvertical to moderately dipping post-cleavage normal faults, of which the larger ones are commonly associated with extensive brecciation, quartz-carbonate veins, and brittle to semi-ductile wall-rock deformation. These faults often have important displacements (~several 100 m) and may have a pronounced effect on the distribution of the different stratigraphic units. Many of these larger faults show evidence of several episodes of fault reactivation. The best examples of these occur within the Nieuwpoort-Asquempont fault zone (De Vos *et al*., 1993a; incorporating the Oudenaarde-Bierghes fault zone of Legrand, 1968 and André & Deutsch, 1985), previously presumed to be a strike-slip fault zone, but recently re-interpreted as a zone consisting of both N- and S-dipping normal faults, deforming the southwestern part of the Brabant Massif into a horst-and-graben geometry (Fig. 2; Debacker *et al*., 2003; 2004b). Normal faulting appears to have been initiated prior to the Givetian conglomerate deposition (Debacker *et al*., 1999), and continued, together with fault reactivation, during the Middle and Late Devonian and later (e.g. Legrand, 1967; Poty, 1991; Debacker *et al*., 1999). Although never observed in outcrop, possibly also the NE-SW-trending faults depicted on the map of De Vos *et al*. (1993a) are post-cleavage normal faults that can be incorporated in this third fault type.

2.2. Correlation with geophysical data

Detailed outcrop observations in the southern part of the Brabant Massif, in combination with high-quality aeromagnetic maps (De Vos *et al*., 1993b; Belgian Geological Survey, 1994), have allowed a correlation of aeromagnetic and field data, thus forming the basis for a geological interpretation of aeromagnetic data in unexposed areas (Sintubin *et al*., 1998; Sintubin, 1999; Debacker, 2001; Debacker *et al*., 2003, 2004a, in press; Piessens *et al*., 2004).

On the aeromagnetic maps, the steep Lower Cambrian core of the Brabant Massif shows up as an aeromagnetic high (De Vos *et al*., 1992, 1993a,b). Modelling of the aeromagnetic signal shows that this aeromagnetic high has a steep architecture, compatible with the structural data (Sintubin & Everaerts, 2002). The SW-limit of this high is formed by the NW-SE-trending aeromagnetic Asquempont lineament (Sintubin & Everaerts, 2002). This lineament, being unrelated to the Asquempont fault (Debacker *et al*., 2003, 2004b), underlies the southwesternmost transition zone between type A folds and type B folds (Debacker *et al*., 2004) and also in the more central and eastern parts of the Cambrian core similar aeromagnetic lineaments coincide with broad zones of type B folds and/or transition zones between type A and type B folds (Fig. 2; Sintubin *et al*., 1998; Debacker *et al*., in press). Like the Asquempont lineament, also these NW-SE-trending lineaments are interpreted as deep-seated, dextral faults or shear zones, of which the displacement at depth is accommodated in a more gradual fashion at the present-day surface by means of folding (Debacker *et al*., 2004a). The dextral sense of movement is based on the Z-shaped geometry of the type B folds and on the cuspate-lobate-shaped, stepwise-displaced southern limit of the aeromagnetic high of the Lower Cambrian core (Fig. 2; Sintubin *et al*., 1998; Sintubin, 1997a,b, 1999; Debacker *et al*., 2004a).

The cuspate-lobate southern limit of the aeromagnetic high has cusps rooting in the NW-SE-trending aeromagnetic lineaments, and lobes, concave to the north, of which the curvature gradually decreases towards the south (Fig. 2). Outcrop observations suggest that the westernmost lobes essentially reflect a buried, steep stratigraphic contact (steep limb of type A fold) between the magnetite-bearing Tubize Formation and the overlying younger deposits (Debacker *et al*., 2004a). Hence, the cuspate-lobate geometry suggests an indentation of the Lower Cambrian core within the Ordovician-Silurian southern part, probably by means of dextral displacement along the NW-SE-trending lineaments, of which the effect gradually diminishes towards the south (Debacker *et al*., 2004a; see also Sintubin *et al*., 1998; Sintubin, 1999; Sintubin & Everaerts, 2002).

Towards the west, the Asquempont lineament coincides with the steep northeastern limit of a negative Bouguer anomaly, reflecting a large, steep-sided low-density body (Fig. 2; De Meyer, 1983, 1984; Everaerts *et al*., 1996). This body, of which the nature is still debated (e.g. De Vos, 1997; Sintubin & Everaerts, 2002), appears to have behaved

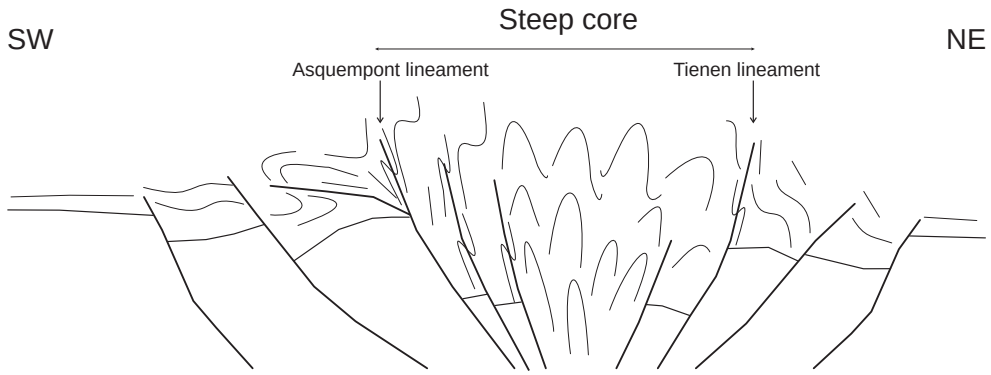

Fig. 3: The core of the Brabant Massif interpreted as a compressional wedge between crustal basement blocks (after Sintubin & Everaerts, 2002). Note that in this model, the low-density gravimetric anomaly body is interpreted as an elevated cratonic basement block (see also Fig. 2).

as a competent body during deformation, judging from its effect on the deformation in its surroundings (Debacker, 2001; Debacker *et al*., 2004a; cf. Sintubin, 1999; Sintubin & Everaerts, 2002). Firstly, to the N and NE of this body, the aeromagnetic contours of the aeromagnetic high mimic its shape. Secondly, the NW-SE-trending aeromagnetic lineaments, of which the southernmost one (Asquempont lineament) coincides with its NE-limit, originate at and converge towards the area to the NE of this body, where its side becomes slightly oblique to the inferred NNE-SSW-directed shortening (Sintubin, 1997a, 1999). Thirdly, its steep NE-side abruptly delimits the steep Lower Cambrian core (Sintubin & Everaerts, 2002). Fourthly, the relatively thin deposits in its roof are deformed by SW-verging, low-angle reverse shear zones (Marcq shear zone, Debacker, 1999), implying an overthrusting of material. Fifthly, the material to the SW of it is undeformed (Verniers & Van Grootel, 1991) (Fig. 2).

Sintubin & Everaerts (2002) interpret the low-density anomaly body as forming part of a cratonic basement block. According to their modelling, cratonic basement blocks are apparent below the rims of the massif but seem absent underneath the Cambrian core. These data lead Sintubin & Everaerts (2002) to consider the Cambrian core of the Brabant Massif as a more or less symmetrical wedge, with a vergence divide, situated between cratonic basement blocks (Fig. 3).

2.3. Progressive deformation and its implications on the timing of deformation

The N-dipping cleavage and the general fold asymmetry in the southern part of the massif suggest a S-verging deformation (e.g. Fourmarier, 1921), which, as demonstrated in several outcrop areas, likely has a progressive nature (Sintubin *et al*., 1998; Debacker, 1999; Debacker *et al*., 1999, 2004a). Furthermore, an integration of field data and geophysical data points to a large-scale deformation history in which the Cambrian core is steepened against the NE-side of the low-density body, parts escape towards the SE, along NW-SE-trending shear zones, and indent the Ordovician-Silurian rim, whereas other parts are thrusted over the roof of the low-density body (Fig. 2). This scenario implies a progressive southward prograding deformation from the core of the massif towards the southern, Silurian rim (Sintubin, 1999; Debacker, 2001; Debacker *et al*., 2004a).

Judging from its progressive nature, deformation did not necessarily take place at exactly the same time in all parts of the Brabant Massif. Considering the southward prograding nature of deformation in the southern part of the massif, from the core towards the Silurian southern rim, the onset of deformation along the Silurian rim is expected to be slightly younger than within the core. Hence, whereas deformation along the Silurian southern rim took place sometime between the Gorstian and the Givetian, as suggested by the angular unconformity, in the Ordovician and Cambrian deposits in the more central parts of the Brabant Massif a slightly older onset of deformation is expected.

3. Constraints on the timing of deformation

3.1. The angular unconformity

At Ronquières, in the southern Sennette valley, the angular unconformity between undeformed, diagenetic Givetian conglomerates of the Bois de Bordeaux Formation (Bultynck *et al*., 1991; Gerrienne *et al*., 2004) and underlying deformed lower Ludlow turbidite deposits of the Ronquières Formation (Gorstian; Louwye *et al*., 1992) indicates a post-early Ludlow to pre-Givetian age for the compressive deformation along the southern rim of the Brabant Massif (cf. Legrand, 1967; Verniers & Van Grootel, 1991; Louwye *et al*., 1992). This rather large hiatus can be further constrained in the western part of the massif, where boreholes show gently dipping Pridoli to lowermost Lochkovian deposits unconformably overlain by sub-horizontal Givetian deposits (Fig. 2; Van Grootel, 1990; Verniers & Van Grootel, 1991).

3.2. Metamorphism along the southern rim

Both the well-developed cleavage, cogenetic with folding (Debacker *et al*., 1999), and the anchizonal degree of metamorphism (Geerkens & Laduron, 1996; Van Grootel *et al*., 1997) in the Gorstian deposits at Ronquières imply the former presence of a significant overburden, which was eroded prior to the deposition of the Givetian conglomerates (cf. Fourmarier, 1921; Legrand, 1967; Verniers & Van Grootel, 1991; Van Grootel *et al*., 1997). The development of a true cleavage fabric, i.e. embryonic cleavage stage of Ramsay & Huber (1983) or higher, necessitates low anchizone conditions (Kisch, 1991; cf. Price & Cosgrove, 1990), thus being compatible with the illite crystallinity data of Geerkens & Laduron (1996). Using an average geothermal gradient of ~36°C/km, as in the Anglia Basin (Merriman *et al*., 1993), the low anchizonal degree of metamorphism of these Gorstian deposits, approximately corresponding to temperatures of 180 to 250°C (Korikovsky & Putis, 1999; Mahlmann, 1996; Merriman *et al*., 1993), suggests a minimum overburden of five kilometres. Higher geothermal gradients of ~50°C/km, as in the Welsh Basin (Tricker, 1992), would suggest an overburden of about four kilometres above the Ronquières Formation. As such, the age of deformation along the Silurian southern rim is controlled by the time necessary for the deposition of the now eroded, minimum 4 km-thick overburden on top of the Ronquières Formation.

3.3. Stratigraphy and subsidence data

Fig. 4 shows a curve of the Lower Palaeozoic stratigraphic

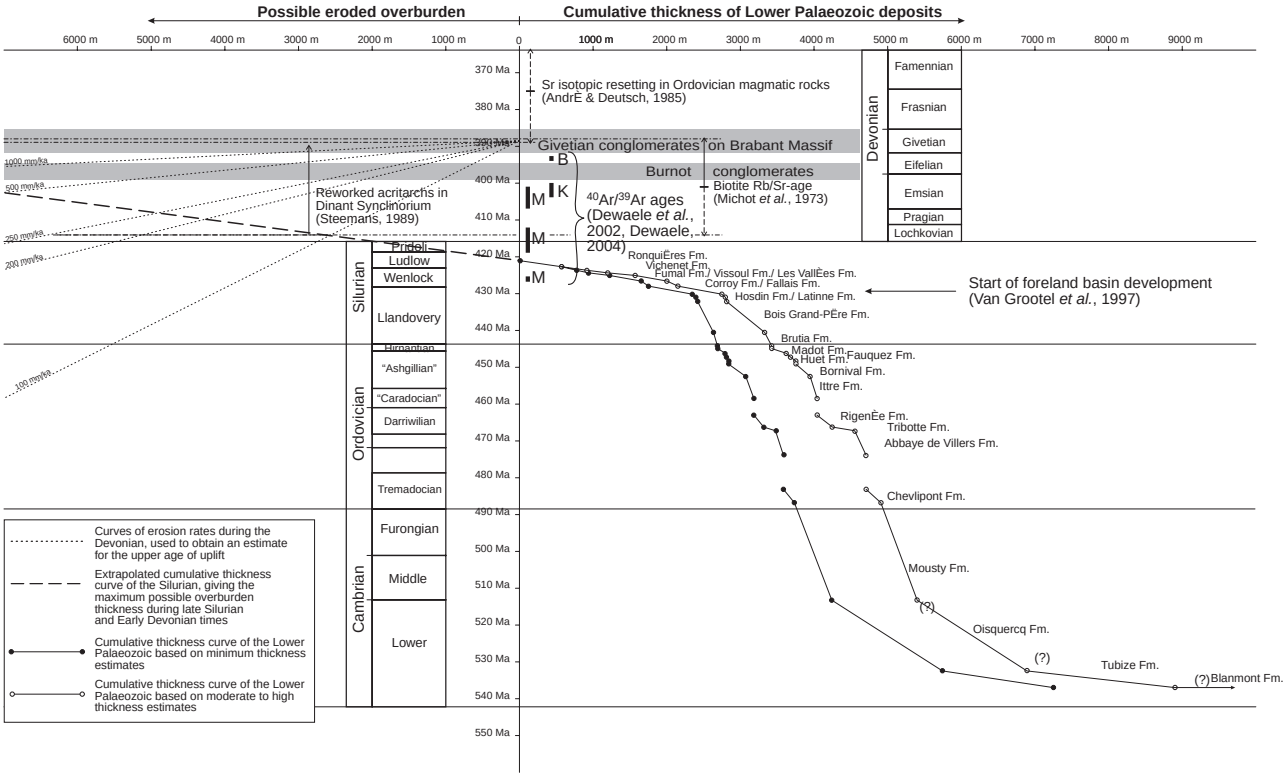

Fig. 4: Cumulative thickness of the Lower Palaeozoic sediments of the Brabant Massif, taken from Verniers *et al*. (2001), plotted against the absolute time-scale of Gradstein *et al*. (2004) (cf. Debacker, 2001). Also shown are radiometric age-ranges of the deformation, taken from Michot *et al*. (1973), André & Deutsch (1985) and Dewaele *et al*. (2002) and Dewaele (2004; M: Marcq; B: Bierghes; K: Kruishoutem). The high rates of sediment thickness against time resulting from Silurian foreland basin development (Van Grootel *et al*., 1997) are extrapolated to higher stratigraphic levels in order to get a maximum value for the age of compressive deformation along the southern, Silurian rim of the massif, taking into account the overburden necessary for cleavage development and metamorphism at given geothermal gradients. A variety of erosion rates is added, of which only those above 250 mm/ka seem feasible, given the conditions during the Early and Middle Devonian. Because of the unspecified age of the Givetian conglomerates unconformably overlying the massif (Bultynck *et al*., 1991), they are placed in the middle Givetian, compatible with recent findings of Gerrienne *et al*. (2004). Since these conglomerates appear to mark the last significant erosion of the Brabant Massif, the origin of the erosion rate curves is placed in the middle Givetian.

thickness, taken from Verniers *et al*. (2001), plotted against the absolute time-scale of Gradstein *et al*. (2004) (cf. Debacker, 2001). Note, that this curve only shows the variation in stratigraphic thickness with time during the Early Palaeozoic, without any thickness corrections for water depth, compaction or tectonic thickness changes (Debacker, 2001). Hence, this curve should not be mistaken with a subsidence curve. Nevertheless, it shows a pattern similar to the subsidence curves of Van Grootel *et al*. (1997). According to the latter authors, the kink in the subsidence curves at the top of the Llandovery, after which rapid subsidence and sedimentation occurs, with the instalment of the Silurian distal turbidite regime, marks the onset of foreland basin development. However, if representing foreland basin development, this implies that by this time a tectonic load was forming within, or in the direct surroundings of, the Brabant Massif.

As argued above, depending on the geothermal gradient, 4 to 5 km overburden was present above the lower Ludlow Ronquières Formation at the time of deformation. Extrapolation of the time-stratigraphic thickness curve towards higher stratigraphic levels, hereby assuming that high sedimentation rates as in the Wenlock-Ludlow continue, indicates that the necessary amount of overburden above the Gorstian deposits along the southern rim of the massif (~4-5 km) cannot have been present prior to the middle Pragian. Taking into account that subsidence and sedimentation rates will decrease once the foreland basin starts to be deformed, with sedimentation rates likely less than that associated with the Wenlock-Ludlow turbidites, the actual deformation along the southern rim will likely have occurred later. Hence, deformation of the Silurian deposits along the southern rim of the Brabant Massif did probably not occur before the late Pragian.

3.4. Distribution of metamorphism

Microstructural observations, illite crystallinity data and the reflectivity of organic matter, led Giese *et al*. (1997; see also Fielitz & Mansy, 1999) to consider the low-grade metamorphism in the Brabant Massif as pre- to early syn-kinematic. More recently, on the basis of illite crystallinity data and K-white mica *b* cell dimension, Larangé (2002) suggested a burial-type metamorphism, confirming the pre-kinematic nature of the metamorphism of Giese *et al*. (1997). Microscopic observations by the present authors are compatible with the results of Giese *et al*. (1997) and Larangé (2002), and suggest that metamorphic conditions were reached during burial, prior to compression, and continued during deformation, only locally extending after deformation. Indications of pre-kinematic metamorphism include the abundance of bedding-parallel chlorite-mica stacks, usually restricted to the microlithons; the presence of crenulated bedding-parallel chlorite-mica stacks; the relationship between chlorite-mica stack aspect ratios and their orientation with respect to cleavage (rounded, almost equidimensional bedding-parallel stacks versus elongated cleavage-parallel stacks); the generally orthorhombic to clear girdle-type chlorite (d002) and white mica (d001) X-ray pole figure patterns, symmetrical about the cleavage/bedding intersection,

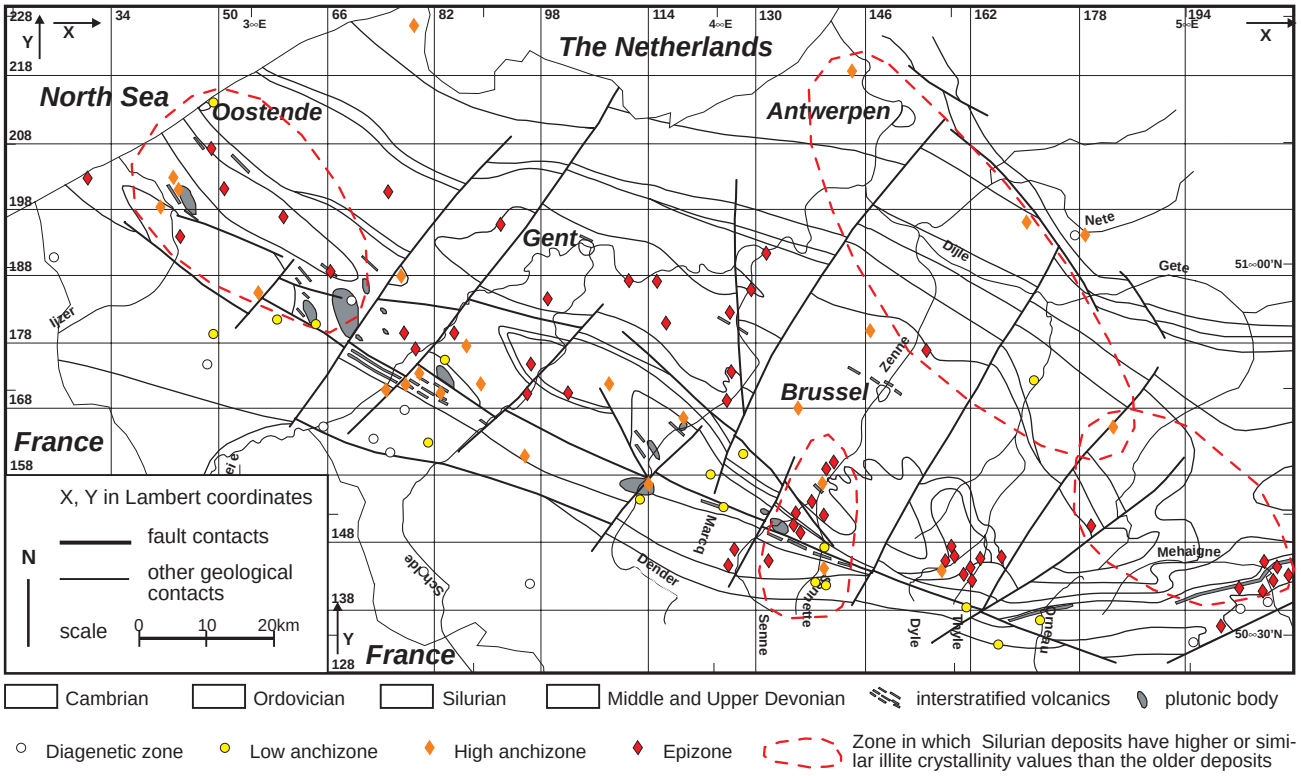

Fig. 5: Geological subcrop map of the Brabant Massif (after De Vos *et al.*, 1993a; Van Grootel *et al.*, 1997) with illite crystallinity data of Geerkens & Laduron (1996; Van Grootel *et al.*, 1997). Note that although in general the highest degrees of metamorphism occur in the Lower Cambrian core, the Silurian deposits often show a relatively high degree of metamorphism with respect to the Ordovician and Upper Cambrian, which is difficult to explain only in terms of burial metamorphism (see also Fig. 6).

implying the superposition of a cleavage fabric on a pre-existing, bedding-parallel, compaction fabric (Debacker *et al.*, 1999; Debacker, 2001; cf. Sintubin, 1994). Indications of syn-kinematic metamorphism include strain shadows filled with chlorite, muscovite and quartz in high strain zones (e.g. Piessens *et al.*, 2002) and indications of late syn-kinematic to post-kinematic metamorphism include chlorite-muscovite slickenfibres on cleavage planes in the Marcq shear zone (Piessens *et al.*, 2002), and the local occurrence of chlorite growing outside of strain shadows along the cleavage in the Lower Cambrian core of the massif.

If the metamorphism is mainly due to burial, the isotherms are expected to be approximately parallel to the stratigraphy, with higher temperatures in the older, Cambrian deposits and lower temperatures along the Silurian rims (cf. Larangé, 2002). However, the cartographic and stratigraphic distribution of the illite crystallinity data of Geerkens & Laduron (1996; cf. Van Grootel *et al.*, 1997) indicates a slightly more complex situation (Fig. 5). Although indeed the highest values are usually obtained in the Cambrian core (epizone), relatively high illite crystallinity values also occur in the Silurian deposits along the rims, with a degree of metamorphism often exceeding that of the Upper Cambrian and Ordovician. In fact, it appears as if the illite crystallinity values decrease from the Cambrian core towards the younger peripheral parts (from epizone to low or high anchizone), but remain the same or slightly increase again in the younger Silurian deposits (anchizone to even epizone; Fig. 6). A comparison with the stratigraphic thickness curves shows that this apparent anomaly, which occurs both in the southern part and in the northern part of the massif, cannot be explained only by the action of a pre-deformation burial metamorphism. One might consider the Ordovician-Silurian magmatism as a cause for the relatively high illite crystallinity values in the Silurian. However, an evaluation of the relative occurrence of magmatism versus the illite crystallinity data shows that

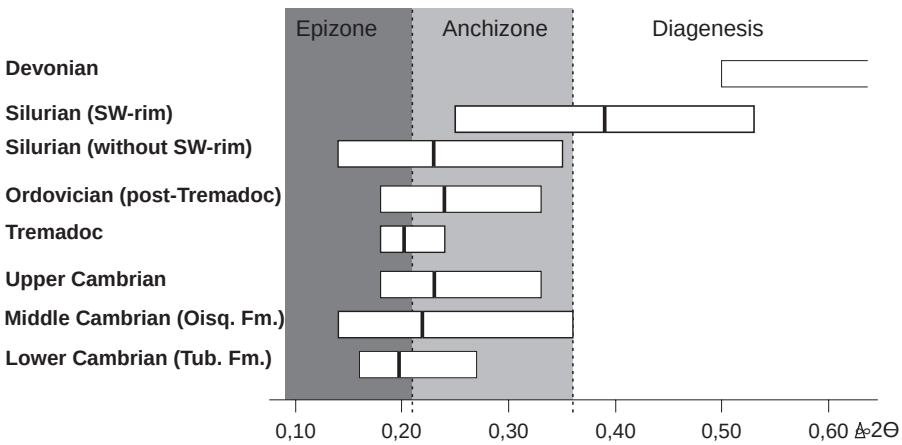

Fig. 6: Graph showing the variation in illite crystallinity (after Geerkens & Laduron, 1996) with stratigraphy (cf. Van Grootel *et al.*, 1997). Note the distinction between the Silurian along the SW-rim of the Brabant Massif (southern rim to the west of the Schelde), essentially being diagenetic to low anchizonal, and the other Silurian deposits, being anchizonal to epizonal. Note the occurrence of epizonal values in the Silurian comparable to or even exceeding those of the Cambrian (Tub.: Tubize; Oisq.: Oisquercq), as well as the absence of a steady decrease in degree of metamorphism between the Upper Cambrian and the Devonian.

this is not likely. Firstly, the main magmatic activity seems to occur between the Caradoc and the Wenlock, with an apparent peak in the latest Ordovician (e.g. Ashgill Madot Formation; Van Grootel *et al.*, 1997; Verniers *et al.*, 2001), whereas the higher metamorphic values usually occur in the overlying, younger rocks. Secondly, also in the northern Silurian rim higher metamorphic values are encountered (Fig. 5). At present, no magmatic deposits have been observed there. Thirdly, in the low-grade, poorly deformed southwestern part of the Brabant Massif, in the direct vicinity of magmatic rocks, very low metamorphic values are observed (Fig. 5). The alternative, and more simple, explanation is to invoke an additional sedimentary load on the rims from the early Silurian onwards, which was much thinner or absent above the Ordovician and Cambrian more central parts of the massif (cf. Debacker, 2001). This hypothesis implies a change in geodynamic conditions from the early Silurian onwards.

3.5. The Givetian conglomerates

The overburden, once present above the Ronquières Formation along the southern rim of the Brabant Massif, was eroded prior to Givetian conglomerate deposition. Taking into account plausible denudation rates, an estimate can be made of the maximum time necessary to erode this overburden, thus allowing a rough estimate of the possible minimum age of deformation.

The proximity to the equator (25 to 15°S, Scotese & McKerrow, 1990), the intensive red colouring of the Givetian conglomerates and the top of the Lower Palaeozoic basement (Legrand, 1967; Mees & Stoops, 1999) and the irregular palaeotopography of the Lower Palaeozoic basement, containing gullies with large quartzitic boulders and thick conglomerate fans, indicate that during the Early to Middle Devonian high erosion rates prevailed. The large quartzitic boulders, locally present in the Givetian conglomerates, are most likely derived from the Lower Cambrian core of the massif, suggesting an advanced stage of unroofing during the Givetian.

These observations suggest that the denudation rates of the Brabant Massif during the Lower and Middle Devonian were most likely higher than 250 mm/ka (cf. Summerfield, 2000). Hence, an overburden of 4 to 5 kilometres could have been eroded easily in less than 18 Ma (Fig. 4), implying that deformation of the southern rim of the massif easily may have occurred as late as middle Emsian.

3.6. Data from the Dinant Synclinorium

The extensive late Emsian to early Eifelian Burnot conglomerates along the northern rim of the Dinant Synclinorium, showing a southward progradational sequence (Godefroid *et al.*, 1994; cf. Corteel *et al.*, 2004) are considered to result from uplift of the Brabant Massif (Michot, 1978; Verniers & Van Grootel, 1991; Corteel & De Paepe, 2003). If the base of these conglomerates corresponds to the initial stage of denudation of the inferred 4-5 km overburden along the southern rim of the Brabant Massif, this denudation should have occurred at rates of approximately 350 to 450 mm/ka for the topography to be levelled by the end of the Givetian conglomerate deposition.

In the Lower Devonian deposits of the Dinant Synclinorium reworked Silurian and Lochkovian acritarchs occur, which are thought to have been derived from the Brabant Massif (Steemans, 1989). In contrast to the Silurian acritarchs within the Brabant Massif, these reworked upper Silurian and Lower Devonian acritarchs do not show evidence of thermal alteration. The stratigraphic distribution of the acritarchs seems to suggest unroofing of the Brabant Massif(?) from the late early Lochkovian onwards (Steemans, 1989). However, although the absence of Cambrian and Ordovician reworked acritarchs derived from the Brabant Massif may be compatible with an initial stage of unroofing, it is very unlikely that the Silurian-Lochkovian acritarchs were derived from the southern rim of the massif, since, as pointed out higher, sedimentation there was likely still going on.

3.7. $^{40}Ar/^{39}Ar$ radiogenic ages

^{40}Ar-^{39}Ar dating was carried out on sericite/muscovite samples taken from different levels in boreholes in the Marcq Area and Kruishoutem, and from the quarry at Bierghes (see Fig. 7 and Tab. 1). It should be noted that macrocrystalline muscovite suitable for dating is very rare in the Brabant Massif. The muscovite samples were handpicked and investigated for their homogeneity by microscopy, SEM analysis and XRD, and identified as very pure muscovite. Minor amounts of quartz can still be found in the samples selected.

At Marcq and Kruishoutem, sericite/muscovite samples have been handpicked from chlorite-muscovite slickenfibers that formed on cleavage planes due to the circulation of metamorphic fluids during cleavage-parallel reverse shearing (Piessens *et al.*, 2002). These slickenfibers are co-genetic with the Cu-Pb-Zn mineralisation, since the deformed ore minerals also occur along the cleavage (Piessens *et al.*, 2002). In the Marcq area, the mineralisation and alteration took place during a protracted simple shear deformation in which cleavage planes are reactivated as shear planes (Piessens *et al.*, 2002). At Bierghes, muscovite occurs microscopically associated with a multistage quartz-carbonate vein system. Vein development, alteration and polysulphide mineralisation in the Bierghes sill have been considered contemporaneous with deformation and occurred after cleavage development (Dewaele *et al.*, 2004). Muscovite was selected from the red alteration stage associated with the quartz-carbonate veins (Dewaele *et al.,* 2004). These veins were ground to a grain size smaller than 1 mm using a jawcrusher and a mortar. The muscovite was concentrated by treating the quartz-carbonate veins with a mild acid. After reaction, the samples were washed with demineralised water. This process was repeated, until no visible reaction between carbonate and acid was observed. The sample was separated in a grain size smaller and larger than 63 μm by sieving. The sample with a grain size > 63 μm was retained for irradiation, because only from this fraction a homogeneous separate of muscovite crystals could be isolated. The fraction < 63 μm was too heterogeneous and the minerals were too small, resulting in a risk of recoil losses of Ar.

Sericite/muscovite is closed for argon loss at a

Sample	Location	Age
19110B7*	Marcq Area	416.1 ± 0.7 Ma
39655B8*	Marcq Area	417.0 ± 1.8 Ma
22995B8*	Marcq Area	404.8 ± 0.8 Ma.
		414.9 ± 3 Ma
16610B6*	Marcq Area	414 ± 1.4 Ma
16785B6*	Marcq Area	414.1 ± 0.5 Ma
18090B6*	Marcq Area	426.1 ± 0.7 Ma
03140C2	Marcq Area	404 ± 3.1 Ma
Bierghes	Bierghes	393.3 ± 0.6 Ma
34300Kr	Kruishoutem	402 ± 1.9 Ma

Table 1: Overview of $^{40}Ar/^{39}Ar$ data of sericite/muscovite from the Brabant Massif. Data with * from Dewaele *et al.* (2002). Sample 34300Kr from Kruishoutem has been taken at a depth of 343m in borehole 84W1386. Marcq area: e.g. sample 19110B7 corresponds to the sample taken at a depth of 191.10m in borehole B7 (114E99), B6 is borehole 114E92, B8 is borehole 114E100 and C2 is borehole 114E102.

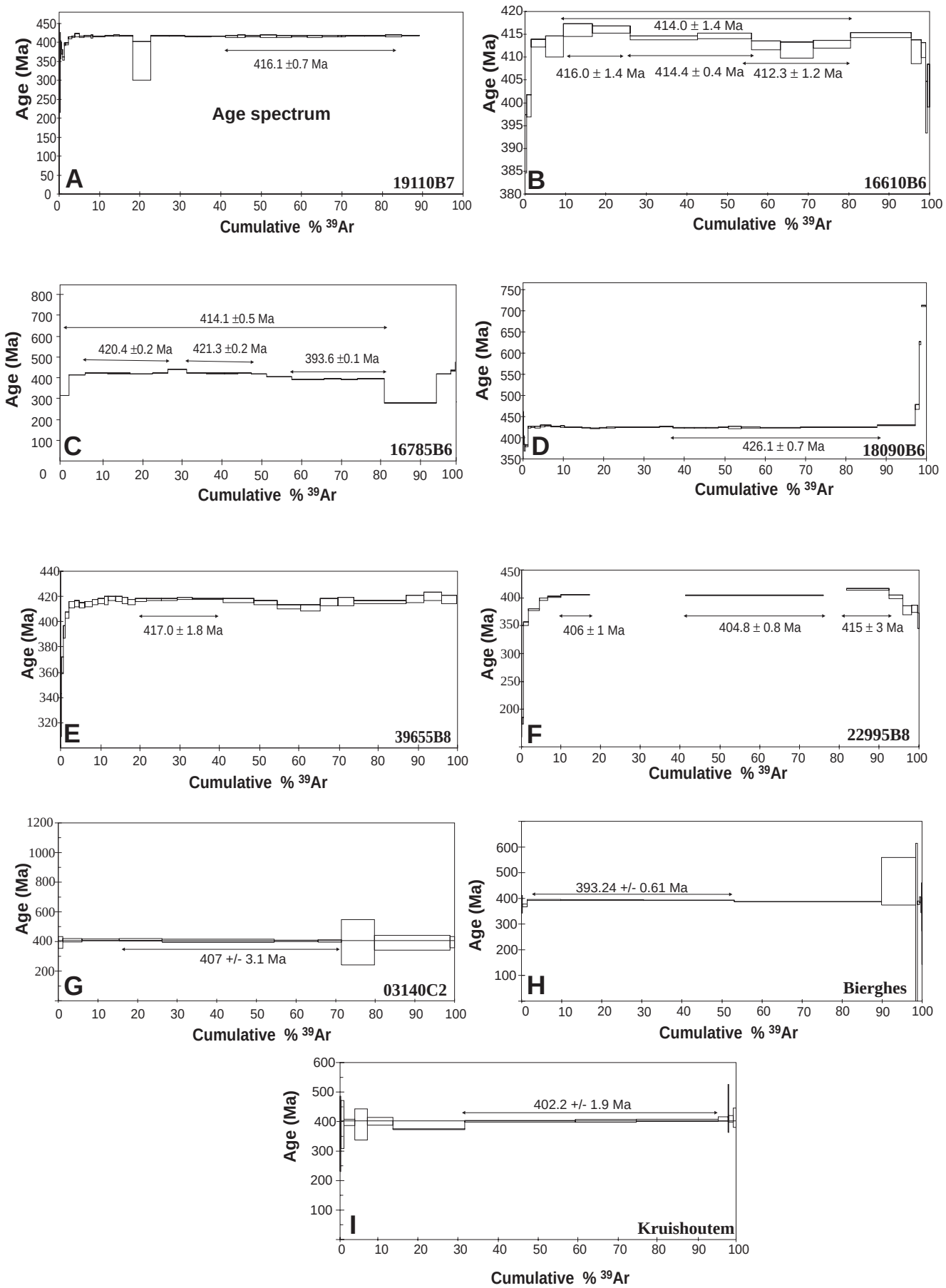

Fig. 7: Results of the $^{40}Ar/^{39}Ar$ data of sericite in the Marcq area (A. 19110B7; B. 16610B6; C. 16785B6; D. 18090B6; E. 39655B8; F. 22995B8; G. 03140C2), Bierghes (H) and Kruishoutem (I). Sample numbers show the depth (in cm) in a borehole, followed by the borehole number (e.g. 19110B7, sample taken at 191.1m in borehole B7). Data from the Marcq area are taken from Dewaele *et al*. (2002).

temperature of ~350°C (e.g. Chesley, 1999). This temperature corresponds to the presumed temperature in the Cambrian core of the Brabant Massif (André & Deutsch, 1985) and to the measured homogenisation temperatures of fluid inclusions in some of the compressive vein systems (Dewaele *et al.*, 2001; Dewaele & Muchez, 2004; Dewaele, 2004). This indicates that the muscovite/sericite grew close to its closing temperature.

These samples, together with aliquots of the LP-6 biotite standard, CaF_2 and K-glass monitors, have been irradiated under Cd-shielding during 3 days in channel E30 in the DG5 carrier of the BR2-reactor of the Belgian Nuclear Research Centre at Mol. Ages are calculated using a J-factor determined from interpolation between 3 J-factors obtained on aliquots of LP-6 biotite for which an age of 128.1 ± 0.2 Ma was used (Baksi *et al.*, 1996). All errors for the ages are given at the 2 σ–level. This accounts for the analytical errors, including the variability of the neutron flux based on dosimetry measurements on a Fe-wire. The analytical details are presented in Boven *et al.* (2001). The uncertainty in the J-factor is ± 1%, but excludes errors on the K and Ca correction factors. Step-wise heating experiments with numerous steps at very small temperature intervals were carried out in a high-vacuum resistance oven, while argon measurements were made on a MAP 216 mass spectrometer operated in static mode. Most samples yield consistent plateau-shaped age spectra and fairly stable Ca/K spectra. Both plateau and total ages, using the percentage of released ^{39}Ar as a weight factor, have been calculated (Dewaele *et al.*, 2002).

Sample 19110B7 yields an excellent plateau age of 416.1 ± 0.7 Ma, which accounts for 70% of the released ^{39}Ar (Fig. 7A). Within error limits, this is equivalent to the plateau age of 417.0 ± 1.8 Ma for sample 39655B8 (Fig. 7E). Sample 22995B8 (Fig. 7F) yields a less regular age spectrum with a staircase increase pattern for the first 20% of released ^{39}Ar. This can be attributed to a loss of radiogenic $^{40}Ar^*$. A next step gives an age of 404.8 ± 0.8 Ma. The highest step age is 415 ± 3 Ma, and is within the error range similar to the age of the two previous samples. Sample 16610B6 at 166.10 m in borehole B6 (Fig. 7B) shows a more disturbed saddle-shaped spectrum. Two consecutive steps yield a highest apparent age of 416.0 ± 1.4 Ma, again similar to previous results. The base of the saddle yields an apparent age of 412.3 ± 1.2 Ma on three consecutive steps. A total fusion age of 414 ± 1.4 Ma, is considered for further interpretation since this corresponds to ~70 % of ^{39}Ar released. The age spectrum for sample 16785B6, at 167.85 m depth in borehole B6 (Fig. 7C), from the most altered part of B6, has a peculiar shape and fluctuations are observed in the Ca/K spectrum. This may be attributed to phase changes occurring during the step-wise heating experiment. A total fusion age of 414 ± 0.5 Ma, is retained for further interpretation as it corresponds to ~80 % of ^{39}Ar released, similar as for 16610B6. However, initial steps correspond to high apparent ages of 421.3 ± 0.2 Ma and 420.4 ± 0.2 Ma and a low apparent age of 393.6 ± 0.1 Ma. The heterogeneity observed in the shape of the individual age spectra could be due to microstructural heterogeneity at the level of the grains as mentioned by Sletten & Onstott (1998), characteristic for shearing activity. Sample 03140C2, at a depth of 31.4 m in borehole C2 (Fig. 7G), gives a plateau age of 407 ± 3.1 Ma for 50 % of the Ar released. This age is clearly younger then the dominant 419-412 Ma range obtained for the other sericites. Sample 18090B6 shows a plateau spectrum with a distinctively higher apparent age of 426.1 ± 0.7 Ma (Fig. 7D). Some excess argon is present in the high temperature steps, but this sample has a very homogeneous Ca/K spectrum and is considered to be a reliable dating. The sericite sample of Kruishoutem yields a plateau age of 402 ± 1.9 Ma, which accounts for 60% of the released ^{39}Ar (Fig. 7I). The sericite sample of Bierghes yields a plateau age of 393.3 ± 0.6 Ma, which accounts for 50% of the released ^{39}Ar (Fig. 7H).

Comparison with Fig. 4 suggests that during the time-interval between 419 and 412 Ma, a maximum overburden of only 1 to 3 km covered the deposits of the Ronquières Formation. Hence, cleavage development within the Ronquières Formation must have occurred later than within the Marcq area, unless one invokes extremely rapid sedimentation during the latest Silurian and Lochkovian and/or unrealistically high geothermal gradients. Furthermore, at ~426 Ma the Ronquières Formation still even had to be deposited.

4. Discussion

4.1. General

A comparison of the data presented above suggests that there is no simple answer for the exact timing of deformation within the Brabant Massif (see Fig. 4). On the one hand, the Burnot conglomerates suggest unroofing during the late Early Devonian. This would be compatible with the biotite Rb/Sr age of Michot *et al.* (1973), with the time necessary for deposition of the inferred overburden along the southern Silurian rim, with the $^{40}Ar/^{39}Ar$ ages from Kruishoutem, with the younger $^{40}Ar/^{39}Ar$ ages of Dewaele *et al.* (2002) from the Marcq area and possibly also with the $^{40}Ar/^{39}Ar$ ages from Bierghes (post-cleavage veins). On the other hand, however, the older $^{40}Ar/^{39}Ar$ ages of Dewaele *et al.* (2002) from the Marcq area suggest an older, late Silurian to early Early Devonian, age of deformation, which is more compatible with the occurrence of reworked acritarchs in the Dinant Synclinorium (Steemans, 1989), and is closer to the onset of foreland basin development (Van Grootel *et al.*, 1997), but is very difficult to reconcile with the deformation of the Silurian southern rim (not enough overburden). Furthermore, there is the inferred onset of foreland basin development during the middle Silurian (Van Grootel *et al.*, 1997), which implies the presence of a growing tectonic load within or in the direct vicinity of the Brabant Massif but which is difficult to link to the other age data summarised above. In addition, also the cartographic and stratigraphic distribution of the illite crystallinity values appears problematic.

Any model for the deformation age of the Brabant Massif should integrate all the data presented and address all the problems outlined above. In particular, it should integrate the progressive nature of deformation, the large-scale structural architecture of the Brabant Massif, the foreland basin development, the stratigraphic and sedimentological data, the metamorphic data and the different radiometric ages.

4.2. Geological significance of the radiometric ages

As outlined above, in the Marcq area (Ordovician) an $^{40}Ar/^{39}Ar$ age has been obtained of 426.1 ± 0.7 Ma. This age corresponds to the middle Wenlock, according to the time-scales of Gradstein & Ogg (1996) and Gradstein *et al.* (2004), and hence pre-dates deposition of the Vichenet Formation (upper Wenlock) and the Ronquières Formation (lower Ludlow; Verniers *et al.*, 2001). Although this age, corresponding to an early stage of foreland basin development, has only been obtained from a single sample and therefore should be interpreted with care, it likely reflects an early stage of hot metamorphic fluid circulation in the Marcq area (Dewaele *et al.*, 2002). These metamorphic fluids are interpreted to have migrated from the Cambrian core, during an early stage of the Brabantian orogeny (Dewaele, 2004; Dewaele *et al.*, 2004; cf. Piessens *et al.*, 2002). Most of the $^{40}Ar/^{39}Ar$ ages in the Marcq area, reflecting the age of newly

formed syntectonic sericite/muscovite, fall between 419 and 412 Ma. These are interpreted as marking the most important period of alteration, deformation and cleavage development in the Marcq area (Dewaele *et al*., 2002). It should be stressed that these ages only hold for cleavage development in the Marcq area and should not be used for the entire massif. For instance, as outlined above, at 419-412 Ma only a small overburden covered the Ronquières Formation, being insufficient to cause the anchizonal metamorphism and the formation of a well-developed cleavage. In the Marcq area and at Kruishoutem, also younger $^{40}Ar/^{39}Ar$ ages (401-407 Ma) have been identified (Dewaele, 2004). Since no excess Ar is considered for these samples (based on homogeneous Ca/K spectra), also these are interpreted as reflecting syn-tectonic metamorphic fluid circulation. The age of 401 to 407 Ma can be reconciled with the Burnot conglomerates and matches the Rb-Sr age on syn-tectonic metamorphic biotite at Opprebais (Michot *et al*., 1973). In addition, by 401-407 Ma, corresponding to the Emsian according to the time-scale of Gradstein *et al*. (2004), an overburden of several km may have accumulated above the Ronquières Formation, sufficient to explain the anchizonal degree of metamorphism (cf. Fig. 4: ~5-7 km overburden?). Hence, the upper Silurian deposits along the southern rim of the Brabant Massif may have experienced cleavage development around 401-407 Ma, coinciding with a later phase of metamorphic fluid circulation at Marcq and Kruishoutem, after cleavage development in the Marcq area (419-412 Ma) and well after the onset of foreland basin development (late Llandovery). Importantly, considering the ages of ~426, 419-412 and 401-407 Ma in the Marcq area, it appears that, at least within the Marcq area, circulation of metamorphic fluids took place episodically during a time-span of at least ~25 Ma.

At Bierghes, sericite has been concentrated from alteration zones associated with quartz-carbonate veins. These veins have a first generation of fluid inclusions with an H_2O-CO_2-(X)-NaCl-KCl composition (Dewaele *et al*., 2004). Total homogenisation temperatures and calculated temperatures from chlorite geothermometry and coexisting sulphide pairs indicate a formation temperature of ~350°C (Dewaele & Muchez, 2004). In the Brabant Massif fluid inclusions with a H_2O-CO_2-(X)-NaCl-KCl composition have a metamorphic origin and formed in a compressive regime (Dewaele & Muchez, 2004; Dewaele *et al*., 2004). Because of this, the ~393 Ma is interpreted as a late metamorphic, post-cleavage, fluid circulation during compressive deformation in the Brabant Massif.

André & Deutsch (1985) interpreted the 373 ± 11 Ma Rb-Sr age in the magmatic rocks at Bierghes, reflecting ^{87}Sr resetting of the intrusive rocks at temperatures of ~250°C, as an indication of Late Givetian strike-slip faulting (end of Frasnian according to the recent time-scale of Gradstein *et al*., 2004). However, judging from André & Deutsch (1985), the proposed strike-slip movement is not based on kinematic evidence, but is merely a deduction, based on the presence of a mylonitic fabric (erroneously claiming that such a fabric cannot form during normal faulting) and on the Middle Devonian stratigraphy of the Namur Basin (a large dip-slip movement should generate a large amount of erosion, which, according to the authors, is not observed). At Bierghes, the zone studied by André & Deutsch (1985) is characterised by a very well developed cleavage (phyllitic), and hence, although we found no evidence for a mylonitic fabric, indeed does represent a high-strain zone. However, we found no kinematic evidence for strike-slip deformation. A large number of poorly developed lineations occur, most of which represent an intersection lineation of cleavage, phyllitic levels and fractures. Within this zone, the only clear lineation evidencing slip consistently has a dip-slip orientation and reflects a normal sense of movement, along the well-developed, pre-existing cleavage (Debacker, 2001). In terms of sense of movement, as well as in terms of position and orientation, this faulting is fully compatible with the normal faults belonging to the Nieuwpoort-Asquempont fault zone (Debacker, 2001; Debacker *et al*., 2003, 2004b). In addition, in post-mineralisation quartz-carbonate veins at Bierghes a fluid with a homogenisation temperature up to 250°C is found (Dewaele & Muchez, 2004). This fluid has an H_2O-NaCl-KCl composition, which is typical for fluids associated with normal faulting along the Nieuwpoort-Asquempont fault zone (Dewaele *et al*., 2004). Therefore, we suggest that the 373 ± 11 Ma obtained by André & Deutsch (1985), being significantly younger than the ~393 Ma post-cleavage $^{40}Ar/^{39}Ar$ age, is related to activity of the Nieuwpoort-Asquempont fault zone, and either reflects normal faulting, or normal faulting-related hydrothermal fluid circulation in the Bierghes sill. Such a Middle to Late Devonian normal fault activity within the Brabant Massif is fully compatible with the results of previous studies (Legrand, 1967; Poty, 1991; cf. Debacker, 2001; Debacker *et al*., 2003, 2004b).

4.3. Proposed deformation history, integrating all data sets

As explained above, the simplest explanation for the illite crystallinity (I.C.) data is to invoke an additional sedimentary load on the rims that was absent above the more central parts of the massif. An easy way to achieve such an additional load is by increasing the subsidence in the rims. Hence, the anomaly in the I.C. data might be related to the strong subsidence starting at the end of the Llandovery, which, according to Van Grootel *et al*. (1997), reflects foreland basin development. The increased subsidence along the rims of the massif from the end of the Llandovery onwards (Van Grootel *et al*., 1997) resulted in a thick sedimentary pile (turbidites), thus giving rise to relatively high I.C. values along both the northern and the southern rim. The rather low I.C. values in the Cambrian core, relative to the comparable values in the Silurian rims, suggest the absence of such an overburden, which may be explained by a relative uplift of the core (Fig. 8). The symmetrical distribution of a Cambrian steep belt bounded both to the north and to the south by Silurian foreland basins suggests that the tectonic load generating foreland basin development may very well have been the rising and deforming Cambrian core itself. This idea is compatible with the compressional wedge model of Sintubin & Everaerts (2002), in which compression caused upward extrusion of the Cambrian core between approaching crustal basement blocks. Hence, it is possible to integrate the large-scale architecture of the Brabant Massif (compressional wedge of Sintubin & Everaerts, 2002), with the foreland basin development along the rims (Van Grootel *et al*., 1997) and with the seemingly anomalous stratigraphic distribution of the degree of burial metamorphism.

In turn, this is compatible with the progressive nature of the deformation and can be reconciled with the different age constraints. As explained in the first part of this paper, the structural and geophysical data point to a southward prograding deformation in the southern part of the Brabant Massif, suggesting that deformation in the Cambrian core may have started earlier than along the Silurian rim. Given the apparent symmetry of the Brabant Massif, inferred from the stratigraphy/sedimentology, the illite crystallinity data (Geerkens & Laduron, 1996; Fig. 5) and geophysical modelling (compressional wedge model with vergence divide of Sintubin & Everaerts, 2002; Fig. 3), a similar scenario may also have occurred in the northern part of the Brabant Massif. This is fully compatible with the idea of the deforming and rising Cambrian core being responsible for Silurian foreland basin development.

The thick Cambrian deposits of the core of the massif are interpreted as being deposited in an extensional basin, possibly a pull-apart basin or a failed rift, between

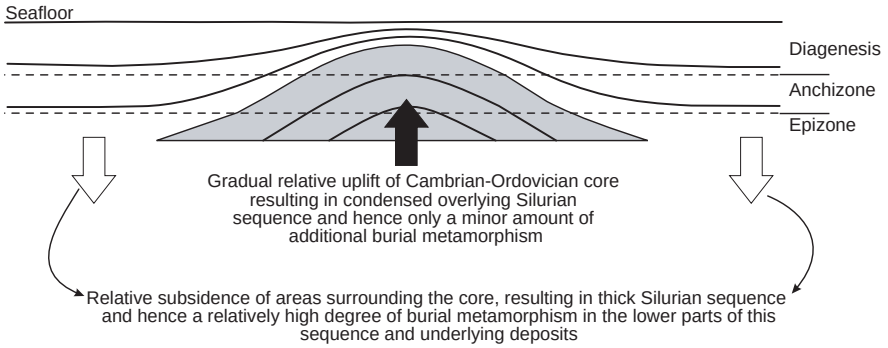

Fig. 8: Model explaining the slight discrepancy between the illite crystallinity (Geerkens & Laduron, 1996) and the stratigraphy. A gradual Late Ordovician – Silurian (?) relative uplift of the Cambrian core of the Brabant Massif results in a condensed Silurian sequence above the central parts and a much thicker Silurian sequence in the subsiding (relative to the core) peripheral parts. In turn, this will lead to only a minor amount of additional burial metamorphism within the Cambrian core of the Brabant Massif, but a relatively high degree of burial metamorphism within the younger peripheral parts.

cratonic basement blocks (Verniers *et al*., 2002; Sintubin & Everaerts, 2002). During initial shortening, the Cambrian core progressively got squeezed out between the approaching cratonic basement blocks, causing the development of a compressional wedge (Sintubin & Everaerts, 2002). The build up of this compressional wedge resulted in a loading of the lithosphere (the same mass on a smaller area), giving rise to foreland basin development along both sides of the Cambrian core (Fig. 9). Considering the time of onset of Silurian foreland basin development, it seems that the Cambrian core was already deforming during the late Llandovery, after which deformation spread progressively from the core towards the rims. The early ~426 Ma $^{40}Ar/^{39}Ar$ age at Marcq (middle Wenlock) is attributed to the circulation of hot metamorphic fluids that were expelled from the deforming Cambrian core, and migrated towards the rims during these early stages of deformation (Dewaele, 2004; cf. Piessens *et al*., 2002). However, although probably deforming since the late Llandovery, with metamorphic fluid migration taking place at least since the middle Wenlock, it is unlikely that the Cambrian compressional wedge emerged prior to the late Ludlow, because of the fact that the Silurian turbidite deposits along the southern rim consistently reflect a southern source area (Verniers, 1983; Verniers & Van Grootel, 1991; Louwye *et al*., 1992). The 412-419 Ma $^{40}Ar/^{39}Ar$ ages, reflecting late Silurian to Lochkovian cleavage development in the low-angle reverse shear zone at Marcq, are interpreted as marking an increment in the progressive spreading of deformation from the Cambrian core towards the Silurian rim. Along the southern Silurian rim, deformation is unlikely to have occurred prior to the late Pragian, for reasons outlined above (cf. Fig. 4). However, around the time of initial cleavage development along the southern Silurian rim, considered to have taken place from the late Pragian or Emsian onwards, also the more internal parts of the Brabant Massif apparently still experienced shortening, as suggested by the post-cleavage metamorphic fluids of 401-407 Ma at Marcq, 402 at Kruishoutem and ~393 Ma at Bierghes. Also the Rb/Sr age of 401 ± 13 Ma of Michot *et al*. (1973), marking new-formation of biotite between the middle Lochkovian and the middle Givetian, is compatible with an extended compressive deformation of the Cambrian core. Probably, if derived from the Brabant Massif, the late Emsian to early Eifelian Burnot conglomerates reflect the first large-scale emersion of the southern part of the Brabant Massif (the core probably emerged already during the Early Devonian), and, together with the ~393 Ma post-cleavage age at Bierghes, likely correspond to the last increments of compressive deformation.

From the reasoning above, it follows that the Brabantian orogeny seems to have lasted for a period of at least ~30 Ma (~430–400 Ma). This inferred long time-span of deformation is in complete agreement with the long time-span of metamorphic fluid circulation evidenced in the Marcq area (~25 Ma; Dewaele *et al*., 2002; Dewaele, 2004).

4.4. Deformation rate

Strain estimates within the outcrop areas of the Brabant Massif on the basis of phyllosilicate X-ray pole figure goniometry (see Sintubin, 1994) suggest a finite shortening in the order of 40 to 60%, mainly resulting from cleavage development (Debacker *et al*., 1999; Belmans, 2000; Debacker, 2001). Only locally, such as within the Marcq shear zone (Piessens *et al*., 2000b) and around the Quenast plug (Debacker, 2001), higher shortening values are obtained, reaching up to ~65%. Judging from these values, the Brabant Massif is unlikely to have experienced a shortening of more than 70%. Assuming a maximum shortening of 70%, during a period of at least 30Ma, a maximum strain rate of $7.4.10^{-16}$/s is obtained for the Brabantian orogeny. This value is significantly lower than conventional tectonic strain rates mentioned in the literature, ranging between 10^{-13} and 10^{-15}/s (Twiss & Moores, 1992; Ribeiro, 2002). Hence, it seems that the Brabantian orogeny was a relatively slow orogeny.

5. Conclusion

The integration of stratigraphic, metamorphic, sedimentological, geophysical and structural data, suggests that the Brabantian orogeny had a long-lived nature, lasting for at least ~30 Ma, from the late Llandovery to the Emsian, possibly even continuing into the Eifelian. This is fully compatible with recent $^{40}Ar/^{39}Ar$ dating (Dewaele *et al*., 2002; Dewaele, 2004), which suggest episodic metamorphic fluid circulation in the Ordovician of the Marcq area during a period of at least ~25 Ma.

We suggest that by the end of the Llandovery, the Cambrian core of the massif was already under compression whereas the Silurian deposits along the rims were still being deposited. This compression caused the build up of a compressional wedge, of which the weight started flexing down the lithosphere, thus giving rise to Silurian foreland basin development on both sides of the Brabant Massif (Fig. 9). During the middle Silurian to early Devonian, this progressive deformation gradually spread towards the Silurian rims of the massif. During this relatively slow, ongoing progressive deformation, metamorphic fluids were episodically expelled prior, during and after cleavage development. Judging from the Silurian sedimentology, it is unlikely that the Cambrian core, progressively deforming since the late Llandovery, emerged prior to the late Ludlow. The Ludlow and younger deposits along the southern rim are considered to have experienced cleavage development after the middle Pragian, and deformation possibly continued into the Eifelian. The Burnot conglomerates likely mark these late increments of deformation. The much younger age of ~375 Ma in Ordovician magmatic rocks, reflecting a Sr-isotopic resetting (André & Deutsch, 1985), is interpreted to be related to normal faulting along the Nieuwpoort-Asquempont fault zone.

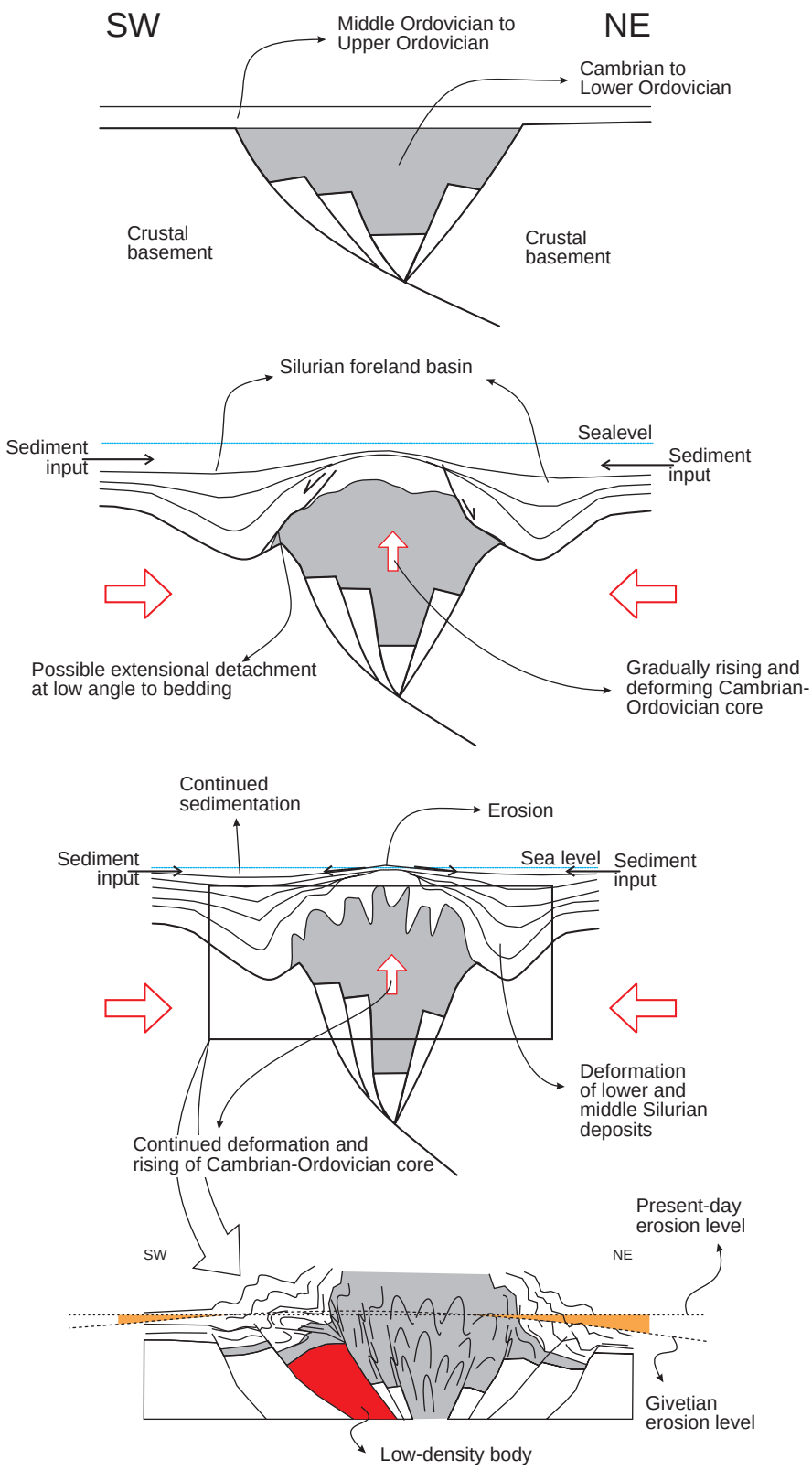

EARLY CARADOC

Basin, possibly a failed rift, filled with Cambrian to Lower Ordovician sediments, overlain by more shallowly deposited Middle Ordovician sediments (cf. Verniers *et al.*, 2002).

WENLOCK

Ongoing inversion of the basin, first affecting the core of the Brabant Massif. The shortening causes a rise of the core, associated with a steepening of the deposits. Silurian foreland basin development is probably the result of the weight of the rising, deforming core. The sediment input is from the south in the southern foreland basin and from the north in the northern foreland basin. The steepening of the core may have caused the development of detachments at low angles to bedding.

LOCHKOVIAN

Continued shortening results in a continued rising and steepening of the core of the massif. The core of the massif emerges, resulting in erosion of the condensed lowermost Devonian and upper Silurian deposits. The northern and southern foreland basins are now completely separated. Continued shortening leads to a spreading of deformation from the core towards the rims.

PRAGIAN TO GIVETIAN

During the Early Devonian continued shortening causes a further spreading of the deformation from the core towards the rims and results in the final inversion of the Silurian to Early Devonian foreland basins during the late Pragian/Emsian, possibly Eifelian. At the same time, also the Cambrian core and the Ordovician experience further, final shortening. Note the lateral changes in thickness of the Silurian deposits. Compare with fig. 3 (modified after Sintubin & Everaerts, 2002).

Fig. 9: Schematic model of the proposed Late Ordovician to Middle Devonian evolution of the Brabant Massif, integrating the stratigraphic, sedimentological, metamorphic, geophysical, geochronological and structural data (not to scale). Following the ideas of Sintubin & Everaerts (2002), the low-density body is shown as an elevated cratonic basement block. Note that this low-density body may also occupy only a part of a cratonic basement block or, alternatively, besides being restricted to the shallow basement block shown, it may also occupy the more deeply buried basement blocks (not visible as low-density bodies because of thick overburden). See text and compare with Figs 1, 2 & 3.

An important implication is that, because of its slow, progressive nature, there is no single exact age for the Brabantian orogeny. The age of deformation will vary from place to place. Only relatively young deformation ages are expected within the late Silurian along the rims (~Pragian - Eifelian), whereas both old and young ages are expected and observed within the older, more central parts of the massif.

6. Acknowledgements

The authors wish to acknowledge P. Ryan and an anonymous reviewer for their constructive remarks on the manuscript. Ph. Claeys is thanked for the stimulating discussion on the results of the $^{40}Ar/^{39}Ar$ analysis. T.N. Debacker is a Postdoctoral Fellow of the Fund for Scientific Research-Flanders (F.W.O.-Vlaanderen) and M. Sintubin a Research Associate of the "Bijzonder Onderzoeksfonds, K.U.Leuven". This work forms part of research projects G.0274.99, G.0094.01 and G.0271.05 of the F.W.O.-Vlaanderen.

References

ANDRÉ, L. & DEUTSCH, S., 1985. Very low-grade metamorphic Sr isotopic resetting of magmatic rocks and minerals: Evidence for a late Givetian strike-slip division of the Brabant Massif, Belgium. *Journal of the Geological Society, London*, 142: 911-923.

ANDRÉ, L., DEUTSCH, S. & MICHOT, J., 1981. Données géochronologiques concernant le développement tectono-métamorphique du segment Calédonien Brabançon. *Annales de la Société Géologique de Belgique*, 104 : 241-253.

BAKSI, A.K., ARCHIBALD, D.A. & FARRAR, E., 1996. Intercalibration of $^{40}Ar/^{39}Ar$ dating standards. *Chemical Geology*, 129: 307-324.

BELGIAN GEOLOGICAL SURVEY, 1994. *Aeromagnetic map of the Brabant Massif: residual total field reduced to the pole. Scale 1/100000.*

BELMANS, M., 2000. *Structurele geologie van het Siluur uit de Orneauvallei, Massief van Brabant*. Unpublished M.Sc.-thesis, Universiteit Gent.

BEUGNIES, A., 1964. Essai de synthèse du géodynamisme paléozoïque de l'Ardenne. *Revue de Géographie Physique et de Géologie Dynamique*, 6 : 269-277.

BOVEN A., PASTEELS, P., KELLEY, S.P., PUNZALAN, L., BINGEN, B., DEMAIFFE, D., 2001. $^{40}Ar/^{39}Ar$ study of plagioclases from the Rogaland anorthosite complex (SW Norway): an attempt to understand argon ages in plutonic plagioclase. *Chemical Geology*, 176: 105-135.

BULTYNCK, P., COEN-AUBERT, M., DEJONGHE, L., GODEFROID, J., HANCE, L., LACROIX, D., PREAT, A., STAINIER, P., STEEMANS, Ph., STREEL, M. & TOURNEUR, F., 1991. Les Formations du Dévonien Moyen de la Belgique. *Mémoires pour servir à l'Explication des Cartes Géologiques et Minières de la Belgique*, 30 : 1-106.

CHESLEY, J.T. 1999. Integrative Geochronology of Ore Deposits : New Insights into the Duration and Timing of Hydrothermal Circulation. . *In*: Lambert, D.D., Ruiz, J. (eds) *Application of Radiogenic Isotopes to Ore Deposit Research an Exploration*. Review in Economic Geology, 12: 115-141.

CORTEEL, C. & DE PAEPE, P., 2003. Boron metasomatism in the Brabant Massif (Belgium): geochemical and petrographical evidence of Devonian tourmalinite pebbles. *Netherlands Journal of Geosciences*, 82: 197-208.

CORTEEL, C., VAN DEN HAUTE, P. & VERNIERS, J., 2004. New sedimentological and petrographical observations on the Devonian Burnot Formation in the Belgian Rhenohercynian basin. *Geologica Belgica*, 7: 41-53.

DEBACKER, T.N., 1999. Folds trending at various angles to the transport direction in the Marcq area, Brabant Massif, Belgium. *Geologica Belgica*, 2: 159-172.

DEBACKER, T.N., 2001. *Palaeozoic deformation of the Brabant Massif within eastern Avalonia, how, when and why?* Unpublished Ph.D.-thesis, Universiteit Gent.

DEBACKER, T.N., 2002. Cleavage/fold relationship in the Silurian of the Mehaigne-Burdinale area, southeastern Brabant Massif, Belgium. *Geologica Belgica*, 5: 3-15.

DEBACKER, T.N., HERBOSCH, A. & SINTUBIN, M. (in press). An alternative model for the thrust fault hypothesis in the Dyle-Thyle outcrop area, southern Brabant Massif, Belgium. *Geologica Belgica*, this vomlume.

DEBACKER, T.N., HERBOSCH, A., SINTUBIN, M. & VERNIERS, J., 2003. Palaeozoic deformation history of the Asquempont-Virginal area (Brabant Massif, Belgium): large-scale slumping, low-angle extensional detachment development (the Asquempont fault redefined) and normal faulting (the Nieuwpoort-Asquempont fault zone). *Memoirs of the Geological Survey of Belgium*, 49: 1-30.

DEBACKER, T.N., HERBOSCH, A., VERNIERS, J. & SINTUBIN, M., 2004b. Faults in the Asquempont area, southern Brabant Massif, Belgium. *Netherlands Journal of Geosciences*, 83: 49-66.

DEBACKER, T.N., SINTUBIN, M. & VERNIERS, J., 1999. Cleavage/fold relationships in the Silurian metapelites, southeastern Anglo-Brabant fold belt (Ronquières, Belgium). *Geologie & Mijnbouw*, 78: 47-56.

DEBACKER, T.N., SINTUBIN, M. & VERNIERS, J., 2001. Large-scale slumping deduced from structural and sedimentary features in the Lower Palaeozoic Anglo-Brabant fold belt, Belgium. *Journal of the Geological Society, London*, 158: 341-352.

DEBACKER, T.N., SINTUBIN, M. & VERNIERS, J., 2004a. Transitional geometries between gently plunging and steeply plunging folds: an example from the Lower Palaeozoic Brabant Massif, Anglo-Brabant deformation belt, Belgium. *Journal of the Geological Society, London*, 161: 641-652.

DE MEYER, F., 1983. Gravity interpretation of the western flank of the Brabant Massif. *Koninklijk Meteorologisch Instituut van België, Publicaties, Serie A/Institut Royal Météorologique de Belgique, Publications, Série A*, 111 : 1-50.

DE MEYER, F., 1984. Two structural models for the western flank of the Brabant Massif. *Geophysical Prospecting*, 32: 37-50.

DE VOS, W., 1997. Influence of the granitic batholith of Flanders on Acadian and later deformation. *Aardkundige Mededelingen*, 8: 49-52.

DE VOS, W., CHACKSFIELD, B.C., D'HOOGE, L., DUSAR, M., LEE, M.K., POITEVIN, C., ROYLES, C.P., VANDENBORGH, T., VAN EYCK, J. & VERNIERS, J., 1993b. Image-based display of Belgian digital aeromagnetic and gravity data. *Professional Paper, Geological Survey of Belgium*, 263: 1-8.

DE VOS, W., POOT, B., HUS, J. & EL KHAYATI, M., 1992. Geophysical characterization of lithologies from the Brabant Massif as a contribution to gravimetric and magnetic modelling. *Bulletin de la Société belge de Géologie*, 101, 173-180.

DE VOS, W., VERNIERS, J., HERBOSCH, A. & VANGUESTAINE, M., 1993a. A new geological map of the Brabant Massif, Belgium. *Geological Magazine*, 130: 605-611.

DEWAELE, S., 2004. *Metallogenesis at the southern margin of the Anglo-Brabant fold belt, Belgium*. Unpublished Ph.D.-thesis, K.U.Leuven.

DEWAELE, S., MUCHEZ, Ph., PIESSENS, K., VANDEGINSTE, V. & BURKE, E.A.J., 2001. P-T-X variation along a polysulphide mineralised low-angle shear zone in the Lower Palaeozoic Anglo-Brabant fold belt (Belgium). *In*: Piestrzynski et al. (eds) *Mineral deposits at the beginning of the 21st Century*. A.A. Balkema, 727-731.

DEWAELE, S., BOVEN, A. & MUCHEZ, PH., 2002. $^{40}Ar/^{39}Ar$ dating of mesothermal, orogenic mineralization in a low-angle reverse shear zone in the Lower Palaeozoic of the Anglo-Brabant fold belt, Belgium. *Transactions of the Institution of Mining and Metallurgy*, 111: B215-220.

DEWAELE, S. & MUCHEZ, PH., 2004. Alteration, mineralisation and fluid flow characteristics in the Bierghes sill, Anglo-Brabant Fold Belt, Belgium. *Geologica Belgica*, 7: 55-69.

DEWAELE, S., MUCHEZ, PH. & BANKS, D., 2004. Fluid evolution along multistage composite fault systems at the southern margin of the Lower Palaeozoic Anglo-Brabant fold belt. *Geofluids*, 4: 341-356. EVERAERTS, M., POITEVIN, C., DE VOS, W. & STERPIN, M, 1996. Integrated geophysical/geological modelling of the western Brabant Massif and structural implications. *Bulletin de la Société belge de Géologie*, 105 : 41-59.

FIELITZ, W. & MANSY, J.-L., 1999. Pre- and synorogenic burial metamorphism in the Ardenne and neighbouring areas (Rhenohercynian zone, central European Variscides). *Tectonophysics*, 309 : 227-256.

FOURMARIER, P., 1921. La tectonique du Brabant et des régions voisines. *Mémoires de l'Académie Royale de Belgique, Classe des Sciences*, 4 : 1-95.

FOURMARIER, P., 1931. Les plissements calédoniens et les plissements hercyniens en Belgique. *Annales de la Société Géologique de Belgique*, 54 : B364-B384.

FOURMARIER, P., 1954. La tectonique. *In*: Michot, P. (ed.) *Prodrome d'une description géologique de la Belgique*, 607-744.

GEERKENS, B. & LADURON, D., 1996. *Etude du métamorphisme du Massif du Brabant*. Unpublished BNRE-report.

GERRIENNE, P., MEYER-BERTHAUD, B., FAIRON-DEMARET, M., STREEL, M. & STEEMANS, P., 2004. *Runcaria*, a Middle Devonian seed plant precursor. *Science*, 306: 856-858.

GIESE, U., KATZUNG, G., WALTER, R. & WEBER, J., 1997. The Caledonian deformation of the Brabant Massif and the Early Palaeozoic in northeast Germany: compared. *Geological Magazine*, 134: 637-652.

GODEFROID, J., BLIECK, A., BULTYNCK, P., DEJONGHE, L., GERRIENNE, P., HANCE, L., MEILLIEZ, F., STAINIER, P. & STEEMANS, P., 1994. Les formations du Dévonien inférieur de la Vesdre, de la Fenêtre de Theux et du Synclinorium de Dinant (Belgique, France). *Mémoires pour servir à l'Explication des Cartes Géologiques et Minières de la Belgique*, 38 : 1-144.

GRADSTEIN, F.M. & OGG, J., 1996. A Phanerozoic time scale. *Episodes*, 19: 3-6.

GRADSTEIN, F.M., OGG, J.G., SMITH, A.G., 2004. *A geologic time scale 2004*. Cambridge: Cambridge University Press.

KISCH, H.J., 1991. Development of slaty cleavage and degree of very-low-grade metamorphism. A review. *Journal of Metamorphic Geology*, 9: 735-750.

KORIKOVSKY, S.P. & PUTIS, M., 1999. Evolution of authigenic and detrital K-micas at the boundary between anchimetamorphism and low-temperature metamorphism during the Cretaceous tectono-metamorphic cycle in the Western Carpathians. *Petrology*, 7: 364-382.

LARANGÉ, F., 2002. *Low-grade metamorphism and geotectonic setting of the Brabant Massif and the medio-occidental part of the Ardenne, Belgium : application of white mica crystallinity, b cell dimension and transmission electron microscope studies*. Unpublished Ph.D.-thesis, Université Catholique de Louvain.

LEGRAND, R., 1967. Ronquières. Documents géologiques. *Mémoires pour servir à l'Explication des Cartes Géologiques et Minières de la Belgique*, 6 : 1-60.

LEGRAND, R., 1968. Le Massif du Brabant. *Mémoires pour servir à l'Explication des Cartes Géologiques et Minières de la Belgique*, 9 : 1-148.

LOUWYE, S., VAN GROOTEL, G. & VERNIERS, J., 1992. The stratigraphy of the type locality of the late Wenlock/early Ludlow Mont Godart Formation and the early Ludlow Ronquières Formation, Brabant Massif, Belgium. *Annales de la Société Géologique de Belgique*, 115 : 307-331.

MAHLMANN, R.F., 1996. The pattern of diagenesis and metamorphism by vitrinite reflectance and illite crystallinity in Mittelbunden and in the Oberhalbstein. 2. Correlation of coal petrographical and of mineralogical parameters. *Schweizerische Mineralogische und Petrographische Mitteilungen*, 76: 23-46.

MEES, F. & STOOPS, G., 1999. Palaeoweathering of Lower Palaeozoic rocks of the Brabant Massif, Belgium: a mineralogical and petrographical analysis. *Geological Journal*, 34: 349-367.

MERRIMAN, R.J., PHARAOH, T.C., WOODCOCK, N.H. & DALY, P., 1993. The metamorphic history of the concealed Caledonides of eastern England and their foreland. *Geological Magazine*, 130 : 613-620.

MICHOT, P., 1976. Le segment varisque et son antécédent calédonien. *Beiträge zur Kenntnis der europäischen Varisziden (Franz-Kossmat-Symposion 1974, Nova Acta Leopoldina). Abhandlungen der Deutschen Akademie der Naturforschungen Leopoldina, N.F.*, 45: 224-838.

MICHOT, P., 1978. La faille mosane et la phase hyporogénique bollandienne, d'âge emsien dans le rameau calédonien condruso-brabançon. *Annales de la Société Géologique de Belgique*, 101 : 321-335.

MICHOT, P., FRANSSEN, L. & LEDENT, D., 1973. Preliminary age measurements on metamorphic formations from the Ardenne anticline and the Brabant Massif (Belgium). *Fortschritte der Mineralogie*, 50 : 107-109.

MORTELMANS, G., 1955. Considérations sur la structure tectonique et la stratigraphie du Massif du Brabant. *Bulletin de la Société belge de Géologie, de Paléontologie et d'Hydrologie*, 64 : 179-218.

PIESSENS, K., DE VOS, W., HERBOSCH, A., DEBACKER, T. & VERNIERS, J., 2004. Lithostratigraphy and geological structure of the Cambrian rocks at Halle-Lembeek (Zenne Valley, Belgium). *Professional Paper, Geological Survey of Belgium*, 300: 1-166.

PIESSENS, K., MUCHEZ, PH., DEWAELE, S., BOYCE, A., DE VOS, W. SINTUBIN, M., DEBACKER, T., BURKE, E. & VIAENE, W., 2002. Fluid flow, alteration and polysulphide mineralisation associated with a low-angle reverse shear zone in the Lower Palaeozoic of the Anglo-Brabant fold belt, Belgium. *Tectonophysics*, 348 : 73-92.

PIESSENS, K., MUCHEZ, PH., VIAENE, W., BOYCE, A., DE VOS, W. SINTUBIN, M. & DEBACKER, T., 2000a. Alteration and fluid characteristics of a mineralised shear zone in the Lower Palaeozoic of the Anglo-Brabant belt, Belgium. *Journal of Geochemical Exploration*, 69-70: 317-321.

PIESSENS, K., VIAENE, W. & MUCHEZ, PH., 2000b. *Metallogenetische studie van gemineraliseerde boorkernen in het Massief van Brabant*. Unpublished final report, ANRE, Project VLA98-3.6.

POTY, E., 1991. Tectonique de blocs dans le prolongement oriental du Massif du Brabant. *Annales de la Société géologique de Belgique*, 114 : 265-275.

PRICE, N.J. & COSGROVE, J.W., 1990. *Analysis of geological structures*. Cambridge: Cambridge University Press.

RAMSAY, J.G. & HUBER, M.I., 1983. *The techniques of modern structural geology; Volume 1: Strain analysis*. London: Academic Press.

RIBEIRO, A., 2002. *Soft plate and impact tectonics*. Berlin: Springer-Verlag.

SCOTESE, C.R. & McKERROW, W.S., 1990. Revised World maps and introduction. *In*: McKerrow, W.S. & Scotese, C.R. (eds) *Palaeozoic Palaeogeography and Biogeography*. Geological Society Memoir, 12: 1-21.

SLETTEN V.W. & ONSTOTT, T.C. 1998. The effect of the instability of muscovite during in vacuo heating on $^{40}Ar/^{39}Ar$ step-heating spectra. *Geochimica et Cosmochimica Acta*, 62: 123-141.

SINTUBIN, M., 1994. Textures in shales and slates. *In*: Bunge, H.J., Siegesmund, S., Skrotski, W. & Weber, K. (eds) *Textures of geological materials*. DGM Informationsgesellsc haft, Verlag, 221-229.

SINTUBIN, M., 1997a. Cleavage-fold relationships in the Lower Paleozoic Brabant Massif (Belgium). *Aardkundige Mededelingen*, 8: 161-164.

SINTUBIN, M., 1997b. Structural implications of the aeromagnetic lineament geometry in the Lower Paleozoic Brabant Massif (Belgium). *Aardkundige Mededelingen*, 8: 165-168.

SINTUBIN, M., 1999. Arcuate fold and cleavage patterns in the southeastern part of the Anglo-Brabant Fold Belt (Belgium): tectonic implications. *Tectonophysics*, 309: 81-97.

SINTUBIN, M., BRODKOM, F. & LADURON, D., 1998. Cleavage-fold relationships in the Lower Cambrian Tubize Group, southeast Anglo-Brabant Fold Belt (Lembeek, Belgium). *Geological Magazine*, 135: 217-226.

SINTUBIN, M. & EVERAERTS, M., 2002. A compressional wedge model for the Lower Palaeozoic Anglo-Brabant Belt (Belgium) based on potential field data. *In*: Winchester, J., Verniers, J. & Pharaoh, T. (eds) *Palaeozoic Amalgamation of Central Europe*. Geological Society, London, Special Publications, 201 : 327-343.

STEEMANS, Ph., 1989. Paléogéographie de l'Eodévonien Ardennais et des régions limitrophes. *Annales de la Société Géologique de Belgique*, 112 : 103-119.

SUMMERFIELD, M.A., 2000. *Geomorphology and Global Tectonics*. Chichester: John Wiley & Sons Ltd.

TRICKER, P.M., 1992. Chitinozoan reflectance in the Lower Paleozoic of the Welsh Basin. *Terra Nova*, 4: 231-237.

TWISS, R.J. & MOORES, E.M., 1992. *Structural Geology*. New York: W.H. Freeman and Company.

VAN GROOTEL, G., 1990. *Litho- en biostratigrafische studie met Chitinozoa in het westelijk deel van het Massief van Brabant*. Unpublished Ph.D.-thesis, Universiteit Gent.

VAN GROOTEL, G., VERNIERS, J., GEERKENS, B., LADURON, D., VERHAEREN, M., HERTOGEN, J. & DE VOS, W., 1997. Timing of subsidence-related magmatism, foreland basin development, metamorphism and inversion in the Anglo-Brabant fold belt. *Geological Magazine*, 134: 607-616.

VERNIERS, J., 1983. The Silurian of the Mehaigne area (Brabant Massif, Belgium), lithostratigraphy and features of the sedimentary basin. *Professional Paper of the Geological Survey of Belgium* 203: 1-117.

VERNIERS, J., HERBOSCH, A., VANGUESTAINE, M., GEUKENS, F., DELCAMBRE, B. PINGOT, J.L., BELANGER, I., HENNEBERT, DEBACKER, T., SINTUBIN, M. & DE VOS, W., 2001. Cambrian-Ordovician-Silurian lithostratigraphical units (Belgium). *Geologica Belgica*, 4: 5-38.

VERNIERS, J., PHARAOH, T., ANDRÉ, L., DEBACKER, T., DE VOS, W., EVERAERTS, M., HERBOSCH, A., SAMUELSSON, J., SINTUBIN, M. & VECOLI, M., 2002. The Cambrian to mid Devonian basin development and deformation history of Eastern Avalonia, east of the Midlands Microcraton: new data and a review. *In*: Winchester, J., Verniers, J. & Pharaoh, T. (eds) *Palaeozoic Amalgamation of Central Europe*. Geological Society, London, Special Publications, 201: 47-93.

VERNIERS, J. & VAN GROOTEL, G., 1991. Review of the Silurian in the Brabant Massif, Belgium. *Annales de la Société Géologique de Belgique*, 114:163-193.

Manuscript received on 29.11.2004 and accepted for publication on 15.11.2005.